1. Konstanty W. MARSZALEK[1] 2. Katarzyna DYNDAŁ[1], 3. Waldemar Szczepanik[2]

AGH University of Krakow, Institute of Electronics (1), Safiro Nutrition Sp. z o.o. sp. K., Wola Dalsza 369, 37-100 Łańcut Poland (2)
1. 0000-0002-0564-5743; ORCID: 2. 0000-0003-2874-5760

doi:10.15199/48.2024.12.39

# Chemical etching for antireflective, gradient n, layer preparation on glass surface

***Abstract**. The paper presents optical properties and applications of a new method of preparing glass plate with anti-reflective properties. In particular, the fabrication of a single-layer anti-reflective system obtained by chemical etching is described. Changes in the optical properties of such a system associated with changes in the thickness of the anti-reflective layer resulting from etching time are shown. A wide range of applications of such a system is presented, resulting from many times lower manufacturing costs.*

***Streszczenie.** W artykule przedstawiono właściwości optyczne i zastosowania nowej metody przygotowania płytki szklanej o właściwościach antyrefleksyjnych. W szczególności opisano wytwarzanie jednowarstwowego układu antyrefleksyjnego otrzymanego metodą trawienia chemicznego. Przedstawiono zmiany właściwości optycznych takiego układu związane ze zmianami grubości warstwy antyrefleksyjnej wynikające z czasu trawienia. Przedstawiono szeroki zakres zastosowań takiego układu, wynikający z wielokrotnie niższych kosztów wytwarzania. **(Trawienie chemiczne jako sposób uzyskania n gradientowych warstw antyrefleksyjnych na szkle)***

**Keywords:** anti-reflective coating, chemical etching, optical properties, transmittance
**Słowa kluczowe:** warstwa antyrefleksyjna, chemiczne trawienie, właściwości optyczne, transmitancja

## Introduction

Anti-reflective coatings on transparent materials, most often applied to utility glass panes and optical elements, are designed to minimize the phenomenon of light reflection from the glass surface. This leads to an increase in the intensity of light transmitted in the entire spectral range from ultraviolet to infrared, or only in the selected spectrum range. This primarily increases the usability of glass and, in the case of optical glasses, the quality and comfort of working with devices that use optics with anti-reflective coatings [1].

Anti-reflective coatings began to be used already during World War II, after developing a technology for applying durable, thin anti-reflective layers on the lenses of binoculars and cameras. Further years brought a rapid development of work on multilayer coatings, which was the result of the development of, among others, vacuum techniques. Currently, ARC (ARC - Antireflective Coating) coatings are commonly used, ranging from glasses to solar panels [2]. Thanks to mass production, there was a significant reduction in production costs, which in turn popularized the use of materials with ARC coating.

The use of renewable energy sources is, in view of the avalanche intensity of adverse phenomena resulting from the use of conventional energy sources, a must. One of the ways to eliminate adverse phenomena, e.g. weather, is certainly the use of solar energy through photovoltaic or photothermal - solar technology [3]. In both these methods of using solar energy, glass is used, whose properties are crucial for the efficiency of devices. Like the thin layers with which solar systems are coated. It is defined in the case of solar cells as a ratio maximum electrical power Pm, obtained from the cell, to the power of solar radiation incident on the Pi cell (1):

(1) $$n = \frac{P_m}{P_i}$$

In the case of photothermal panels - heating utility water, the definition is analogous. The phenomenon of reflection of some radiation from the glass surface reduces the intensity of transmitted light and thus the efficiency of the entire device. This is especially important in countries in a moderate climate zone (i.e. in Europe) due to the fact that for a significant part of the year the sun is low above the horizon and the small angle of incidence of light causes significant energy loss due to light reflection from the glass surface. The situation becomes doubly unfavorable in winter periods when the angle of incidence of light is the smallest and the amount of energy reaching from the sun is small. Under these conditions, the percentage of use of this energy is the lowest, although this energy is most needed during these periods. This effect can be minimized by using turntables that follow the Sun for some devices, but this solution has a serious disadvantage - the installation is no longer maintenance-free and becomes more emergency. In addition, turntables can only be used in principle for solar panels. Their use for heating collectors is difficult due to the large weight of the collector, and in the case of greenhouses such a solution is impossible to apply.

The principle of operation of anti-reflection coatings is based on two phenomena.

If a layer with an intermediate refractive index value is installed on the border of two optical centers with different refractive index values (glass and air), the light reflection index from this limit will decrease. It is possible to select the refractive index of the coating layer such that the reflection coefficient is as low as possible.

When applying a coating layer of appropriate thickness, the rays reflected from both border surfaces of the layer will be extinguished due to interference.

The reflection coefficient is the ratio of the reflected wave intensity to the incident wave intensity (2):

(2) $$R = \frac{I_0}{I_p}$$

where: $I_0$ - incident wave intensity, $I_p$ - reflected wave intensity.

Reflection coefficient is a function of the angle of incidence For light, this relationship results from the Fresnel formulas for the Fresnel reflection coefficient RF. The relationship between the reflection coefficient and the angle of incidence is expressed by the formula (3):

(3) $$R = \left(\frac{n\cos\beta - \cos\alpha}{n\cos\beta + \cos\alpha}\right)^2$$

where:
α - light incidence angle, β - refraction angle, n - the relative refractive index of the medium from which the light reflects relative to the medium in which the light first propagates.

By creating a coating on the glass surface (by any method) with a properly selected layer thickness and an appropriate refractive index, you can reduce or increase the reflection coefficient for different wavelengths of radiation incident on the glass surface. The way the electromagnetic wave is reflected at the interface between the air-ARC layer and the ARC-glass layer is presented in Figure 1.

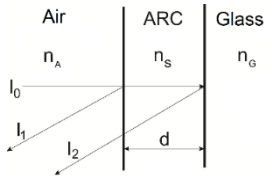


Fig. 1. Reflection diagram for the electromagnetic wave at the air-ARC layer interface, ARC-glass layer.

According to the diagram in Figure 1 for a specific wavelength λ, the reflected light intensity is expressed by equation (4):

(4) $$I_r = I_1 + I_2 + 2\sqrt{I_1 I_2}\, cos 4\pi \frac{n_s d}{\lambda}$$

To reduce the reflected light to zero, the following conditions must be met (5) and (6):

(5) $$d = \frac{\lambda}{4n_s}(2k+1)$$

(6) $$I_1 = I_2$$

because then (7):

(7) $$I_r = I_1 + I_2 - 2\sqrt{I_1 I_2} = 0$$

In practice, it is assumed that the refractive index of the ARC layer should be the geometric mean of the refractive index of both media, i.e. air and glass, and the thickness of the ARC layer should be equal to ¼ of the wavelength whose reflection is to be suppressed.
Another phenomenon to consider is the interference of radiation reflected from boundary surfaces. This phenomenon, with properly selected parameters of the ARC layer, can eliminate the phenomenon of iridescence.
In a linear medium, the disturbances originating from several sources meet at a given point P. The disturbance of this medium at this point is the sum of the disturbances caused by individual waves. In the simplest case of two harmonic waves of equal amplitudes A, equal wavelength λ and compatible initial phases, diverging from two different sources, which lie at distances $d_1$ and $d_2$ respectively from point P, the disturbance at point P is described by the formula (8):

(8) $$y(P) = A\, sin(\omega t + \varphi_1) + A sin(\omega t + \varphi_2$$

where: $$\varphi_1 = \frac{d_1}{\lambda},\ \varphi_1 = \frac{d_1}{\lambda}$$

In the event that: $\varphi_1 - \varphi_2 = 2k\pi$

where: k - any natural number (0, 1, 2 ...) then the waves at point P are amplified and (9):

(9) $$y(P) = 2A\, sin(\omega t)$$

However, when (10):

(10) $$\varphi_1 - \varphi_2 = (2k+1)\pi$$

waves are blanking and y (P1) = 0.

Monolayer coatings are used primarily in the solar industry due to the very wide range of operation (it is possible to increase the transmittance in almost the entire range of solar spectrum emission). This is very important because most of the devices using solar energy use relatively wide bands (e.g. silicon-based photovoltaic cells from ultraviolet to near infrared (although the latter is most efficient), collectors heating water throughout the entire radiation range, greenhouses like chlorophyll - from ultraviolet up to and including red light).

Multilayer coatings are not used in the solar industry for two reasons. Firstly, to obtain a wide range of anti-reflective properties (at least several hundred nanometers), it is necessary to use a coating with very many layers, and hence relatively expensive. Secondly, such coatings are exposed to continuous exposure to changing weather conditions. This can cause damage to the coating (delamination due to the difference in temperature expansion of the layers), cracking, corrosion), whereby the problem increases as it moves towards the poles (damaging effects of freezing water), in warm and dry countries, anti-reflective coatings degrade very slowly. Monolayer coatings are also most often applied to the glass surface and face similar problems. However, technologies are used that allow obtaining an anti-reflective layer, which is not an applied coating.

Selective etching of the glass surface helps give it anti-reflective properties. The thickness of the anti-reflective layer can be controlled by the etching time. Tracking how the transmittance increases with the thickness of the layer makes it possible to estimate its thickness. Additional confirmation of its thickness is provided by measuring the transmittance at different angles of incidence of the light beam. When the layer is thinner than ¼ wavelength, at a slight angle the transmittance should increase instead of decrease. Similarly, when the thickness of the layer exceeds ¼ lambda, the transmittance should decrease regardless of the angle of incidence of the light beam (as the thickness of the layer approaches ½ lambda, the transmittance decreases, only to increase again for a thickness of ¾). Thus, two phenomena can be observed: an increase in transmittance as the antireflective layer increases, and a shift of the transmittance maximum toward longer wavelengths (from violet light toward blue light, then green and red light). This is a very big advantage of the described technology because it allows to place the transmittance maximum exactly where it will bring the greatest benefit (e.g. PV panel - near infrared, greenhouse - visible range + near ultraviolet (photosynthetically active range).

This work presents one method of increasing the transmittance of glass, which involves chemically etching its surface with acid. The results of the transmittance of the etched glass at different times, as well as for different angles of incidence of light, were presented. The thicknesses of the etched layers, refractive indices and extinction coefficients were also determined.

**Materials**

Glass slides made of sodium-calcium glass with a chemical composition of $SiO_2$ (72.7%), $Na_2O$ (13%), CaO (8.8%), MgO (4.3%), $Al_2O_3$ (0.6%), $K_2O$ (0.4%), $SO_3$ (0.2%), and $Fe_2O_3$ (0.2%) were utilized in the study. These glass slides were manufactured by Nippon Steel Glass and measured 5 cm by 5 cm in dimension with a thickness of 4 mm. The refractive index of the glass as declared by the manufacturer was 1.52 for a wavelength of 589 nm [4].

**Methods**

To modify the optical properties of the glass, it was chemically etched using hexafluorosilicic acid ($H_2SiF_6$). The thickness of the etched layer was controlled by using different modification times.

Spectroscopic studies were carried out using an Avantes Sensline Ava-Spec ULS-RS-TEC fiber optic spectrophotometer (Avantes, Appelsdorn, the Netherlands) with an AvantesAvaLight DH-S-BAL lamp and an integrating sphere.

The refractive index (n) and extinction coefficient (k) were determined by spectroscopic ellipsometry. This technique is very accurate, non-destructive, and particularly suitable for analyzing thin films [5, 6]. In this method, the polarization state of the light reflected from the sample is measured, and the polarization is represented in terms of ellipsometric angles Psi (Ψ) and Delta (Δ) as a function of the wavelength of the light determined for different angles of incidence [7].
By knowing the values of Ψ and Δ, the thickness and optical constants of the layers can be determined by fitting an appropriate optical model [8, 9]. The ellipsometric measurements were carried out using the M-2000 J.A. spectroscopic ellipsometer from Woollam Co., Inc. The angles Ψ and Δ were measured at angles of incidence of 65, 70, and 75° in spectral ranges from 350 to 1700 nm.
The spectral dependencies of Ψ(λ) and Δ(λ) were fitted using the Sellmeier model used for transparent dielectric materials given by the equation (11):

(11) $$\epsilon(\lambda)_1 = n(\lambda)^2 = 1 + \frac{A\lambda^2}{\lambda^2 - {\lambda_o}^2}$$

where: ε is the dielectric function, n is the refractive index, λ is the wavelength (in nm), A is the amplitude and $\lambda_o$ is the resonance wavelength [10].

The Complete EASE 5.08 software was used to perform all calculations, allowing for the determination of refractive index, n(λ), extinction coefficient, k(λ), and layer thickness (d). To evaluate the model fit to the experimental data, the criterion of minimizing the mean square error (MSE) was applied, which takes into account the differences between the measured values and those obtained from the model, as well as the standard deviations for each wavelength [11].

To determine the thickness and optical constants, a model of layers obtained during the etching process was proposed. The model assumes that etching induces a gradient change in the refractive index, and this change is linear with respect to the depth of the etching agent's action [9]. For the best fit of the model to the measurement results, the modified area was divided into two layers, with a gradual change in the refractive index. A simplified diagram illustrating the proposed model of chemically etched glass is shown in Figure 2. The refractive index value n corresponds to the refractive index of the unetched glass. Refractive index values $n_1$ and $n_2$, as well as $n_3$ and $n_4$, pertain to the most inner and outer gradient layers, respectively, with their values changing linearly from $n_1$ to $n_2$ and from $n_3$ to $n_4$ (Fig. 2).

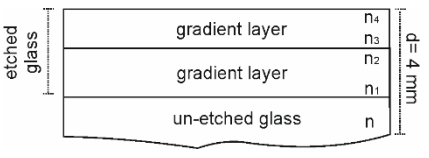


Fig. 2 Model of a glass sample treated with chemical etching

## Results and Discussion

### *Transmittance studies*

The transmittances of the obtained antireflective layers of different thicknesses were measured and controlled by etching time. Example results from the measurements are shown in Figure 3.

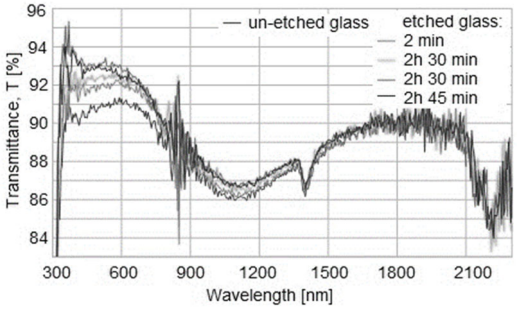


Fig. 3 Increase of glass plate transmittance as a function of anti-reflective layer thickness resulting from etching time

As the etching time increases, the transmittance of the layers increases. The maximum transmittance obtained for the etched layers was about 96% (Fig.4), which is about 6% higher than for commercial glasses. The increase in transmittance is seen first in the near ultraviolet and blue light range because shorter wavelengths are absorbed strongly by the etched material. Another observed phenomenon probably caused by the increase in thickness of the antireflective layer is a shift in transmittance toward green light (Fig. 4).

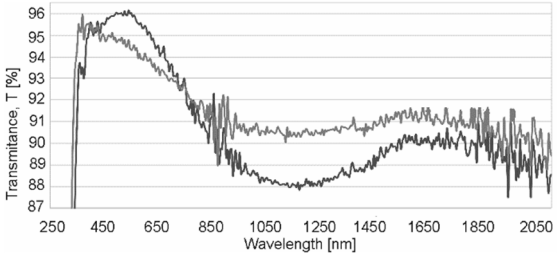


Fig. 4. Maximum transmittance shift due to increase in thickness antireflective layer

Tracking how the transmittance increases with the thickness of the layer allows estimating the thickness of the layer. Additional confirmation is provided by measuring the transmittance at different angles of incidence of the light beam. When the layer is thinner than ¼ wavelength, at a slight angle the transmittance should increase instead of decrease. Similarly, when the thickness of the layer exceeds ¼ lambda, the transmittance should decrease regardless of the angle of incidence of the light beam (as the thickness of the layer approaches ½ lambda, the transmittance decreases, only to increase again for a thickness of ¾). Thus, two phenomena can be observed: an increase in transmittance as the antireflective layer increases, and a shift of the transmittance maximum toward longer wavelengths (from violet light toward blue light, then green and red light). This is a very big advantage of the described technology because it allows to place the transmittance maximum exactly where it will bring the greatest benefit (e.g. PV panel - near infrared, greenhouse - visible range + near ultraviolet (photosynthetically active range). Conclusions regarding the thickness of the anti-reflective layer can also be drawn from the analysis of transmittance for different angles of incidence of the light beam on the sample. Transmittance should be highest when the light falls perpendicular to the sample and decreases as the angle of incidence increases. An interesting phenomenon of transmittance increase for small angles of incidence of light beam can be observed for samples whose anti-reflective layer did not reach the value of ¼ lambda. This is illustrated in Table 1. It is unexpected that even for an angle of incidence of light beam 30 degrees, the transmittance is still greater than for a right angle.

Table 1. Results of hemispherical measurement of transmittance of a sample whose anti-reflective layer did not reach ¼ lambda thickness

| The angle of incidence [°] | | | | | |
|---|---|---|---|---|---|
| 0 | 15 | 30 | 45 | 60 | 90 |
| Transmittance [%] | | | | | |
| 92.390 | 92.981 | 93.099 | 92.780 | 88.080 | 0.000 |

Transmittance values for a sample whose antireflective layer thickness exceeded ¼ lambda are presented in Table 2. Transmittance decreases as the angle of incidence increases. The results presented in the tables show one of the significant advantages of chemically etched anti-reflective layers, i.e. increased system transmission even for large electromagnetic radiation angles.

Table 2. Transmittance of the sample whose anti-reflective layer exceeded the optimal thickness

| The angle of incidence [°] | | | | | |
|---|---|---|---|---|---|
| 0 | 15 | 30 | 45 | 60 | 90 |
| Transmittance [%] | | | | | |
| 93.49 | 93.029 | 92.330 | 90.758 | 85.437 | 0.000 |

**Ellipsometric studies**

The refractive index (n) of chemically etched glass gradually decreases with depth. The refractive index decreases from n=1.52 for unetched glass to $n_4$=1.38 for the most outer etched surface (the interface between the etched glass and air). The refractive indices for the individual interface surfaces shown in Figure 2 are respectively n=1.52, $n_1$=1.52, and $n_2$=1.42 (Fig. 5a), and $n_3$=1.42 and $n_4$=1.38 (Fig. 5b) for a wavelength of 633 nm.

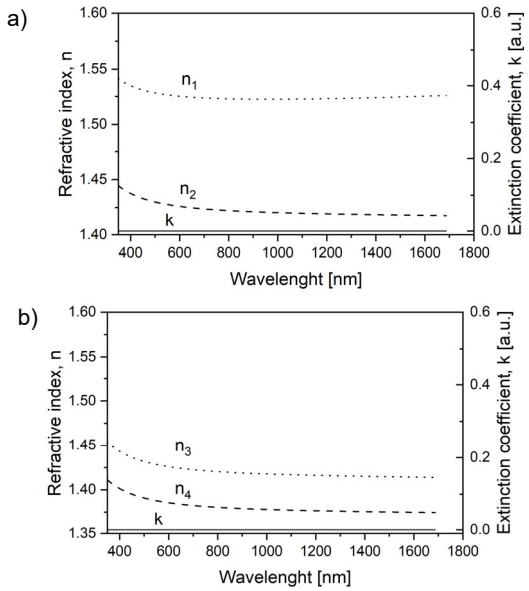


Fig. 5. Refractive index and extinction coefficient determined for gradient layers bordering (a) untreated glass ($n_1$, $n_2$) and (b) bordering air ($n_3$ and $n_4$)

The extinction coefficient over the entire wavelength range was zero. The determined thicknesses of the gradient layers after etching were 23.5 nm and 38.7 nm for the outermost layer (bordering the air) and the inner layer (bordering the non-etched glass), respectively (Fig. 2).

The determined values of n, k and d were determined when fitting the model to experimental data with MSE=1.45.

**Conclusions**

The paper presents the applications of anti-reflective coatings. Specifically, it describes a method of fabrication a low-cost, single-layer anti-reflective system through the use of chemical etching. The method of modifying the glass properties resulted in a high transmittance value of 96%, which is 6% higher than that of unmodified glasses. Additionally, the coatings exhibited high transmittance even for light incident at various angles. The optical characteristics of the coatings presented are extremely interesting from an application perspective. This is particularly important, for example, in greenhouses and photovoltaic systems.

***Acknowledgments***

*Research project supported by program "Excellence initiative – research university" for the AGH University of Science and Technology (project no. 4121).*

***Authors**: dr hab. inż. Konstanty W. Marszalek, prof. AGH, AGH University of Krakow, Institute of Electronics, Al. Mickiewicza 30, Kraków, Poland, E-mail: marszale@agh.edu.pl;dr inż. Katarzyna Dyndał, AGH University of Krakow, Institute of Electronics, Al. Mickiewicza 30, Kraków, Poland, E-mail: kkoper@agh.edu.pl; Waldemar Szczepanik, Safiro Nutrition Sp. z o.o. sp. K., Wola Dalsza 369, 37-100 Łańcut, Poland, E-mail: w.szczepanik@safironutrition.com*

REFERENCES

[1] M. Lorens et al., "Micropatterning of silicon surface by direct laser interference lithography," Acta Phys. Pol. A, vol. 121, no. 2, pp. 543–545, 2012, doi: 10.12693/APhysPolA.121.543.

[2] K. Marszałek, P. Winkowski, and J. Jaglarz, "Optical properties of the $Al_2O_3/SiO_2$ and $Al_2O_3/HfO_2/SiO_2$ antireflective coatings," Mater. Sci. Pol., vol. 32, no. 1, pp. 80–87, 2014, doi: 10.2478/s13536-013-0156-y.

[3] G. Wroblewski et al., "Graphene platelets as morphology tailoring additive in carbon nanotube transparent and flexible electrodes for heating applications," J. Nanomater., vol. 2015, pp. 1–8, 2015, doi: 10.1155/2015/316315.

[4] NSG-Group, "Technical Bulletin, Properties of soda-lime silica float glass," Toledo, Ohio, 2013.

[5] K. Dorywalski and A. Patryn, "Technika elipsometrii spektroskopowej jako metoda monitorowania jakości powierzchni materiałów grupy SrxBa1-xNb2O6," Przegląd Elektrotechniczny, vol. R. 90, nr, pp. 22–25, 2014.

[6] G. Lewińska et al., "Investigation of dye dopant influence on electrooptical and morphology properties of polymeric acceptor matrix dedicated for ternary organic solar cells," Polymers (Basel)., vol. 13, no. 23, 2021, doi: 10.3390/polym13234099.

[7] D. S. S. Almeida et al., "Ellipsometric characterization of surface films on AZ31 magnesium alloy exposed to a Na2SO4 solution," J. Mater. Res. Technol., vol. 9, no. 5, pp. 10175–10183, 2020, doi: 10.1016/j.jmrt.2020.07.030.

[8] J. N. Hilfiker, J. A. Woollam, and M. R. Linford, "Using Interference Enhancement to Increase the Information Content of Spectroscopic Ellipsometry Measurements," Vac. Technol. Coat., no. August, 2022, [Online]. Available: www.vtcmag.com

[9] J. Jaglarz, T. Wagner, J. Cisowski, and J. Sanetra, "Ellipsometric studies of carbazole-containing polymer layers," Opt. Mater. (Amst)., vol. 29, no. 7, pp. 908–912, 2007, doi: 10.1016/j.optmat.2006.02.003.

[10] G. E. Jellison, T. Aytug, A. R. Lupini, M. P. Paranthaman, and P. C. Joshi, "Optical properties of a nanostructured glass-based film using spectroscopic ellipsometry," Thin Solid Films, vol. 617, pp. 38–43, 2016, doi: 10.1016/j.tsf.2015.12.046.

[11] D. Ngo et al., "Spectroscopic ellipsometry study of thickness and porosity of the alteration layer formed on international simple glass surface in aqueous corrosion conditions," npj Mater. Degrad., vol. 2, no. 1, pp. 1–9, 2018, doi: 10.1038/s41529-018-0040-7.